PERGAMON Mathematical and Computer Modelling 29 (1999) 11–30

MATHEMATICAL AND COMPUTER MODELLING

Directly Transmitted Infections Modeling Considering An Age-Structured Contact Rate—Epidemiological Analysis

H. M. YANG
Universidade Estadual de Campinas
IMECC, Depart. Matem. Aplicada
Caixa Postal 6065, CEP: 13081 970; Campinas, São Paulo, Brasil
hyunyang@ime.unicamp.br

(Received and accepted December 1998)

Abstract—Many directly transmitted diseases present a strong age dependent pattern of infection. Such dependency is analyzed by a mathematical model encompassing an age-structured pattern of contacts. From an age-structured contact rate modeling, we estimate the parameters related to the contact rate based on the age dependent force of infection calculated from a seroprevalence data obtained from a nonimmunized population.

This model, with parameters completely determined, is used to assess the effects of vaccination strategies. This is done by calculating the new equilibrium age dependent force of infection and its correlated variables: the average age of the acquisition of the first infection, the rate of new cases of infection, and the risk of Congenital Rubella Syndrome. Also, we present a rough estimation of the *basic reproduction ratio* and the vaccination rate at which the disease can be considered eradicated (threshold).

Keywords—Age-structured contact rate, Threshold, Vaccination, Epidemiological parameters.

1. INTRODUCTION

In a previous paper [1], we presented a theoretical framework to deal with the spread out of directly transmitted infections, developing an age-structured pattern of contacts among individuals in the community. From this pattern of contacts among individuals, we obtained an age-structured contact rate taking into account the transmissibility (infectivity) of virus.

However, when dealing with a constant contact rate modeling, there are classical results related to the *basic reproduction ratio* and the lower value (threshold) for the vaccination rate above which the disease can be considered eradicated. These results are easily estimated from real data. With respect to age-structured modeling, there are also well-defined results related to the basic reproduction ratio R_0 and the threshold vaccination rate. For instance, Greenhalgh [2] and Inaba [3] showed the existence and uniqueness of the nontrivial solution for the Hammerstein equation similar to that presented in [1]. They showed that the bifurcation from the trivial to nontrivial solution of the Hammerstein integral equation occurs when the spectral radius assumes unity value. Furthermore, they related this spectral radius with the basic reproduction ratio, and

Partially supported by FAPESP Grant # 97/12543-4.

0895-7177/99/$ - see front matter. Typeset by $\mathcal{A}\mathcal{M}\mathcal{S}$-TEX
PII: S0895-7177(99)00059-X

stated that whenever $R_0 < 1$, the disease is not able to establish in the community, and when $R_0 > 1$, then the disease can be settled at an endemic level. Following the same arguments, they showed the procedure to calculate the threshold vaccination rate.

In the present paper, we deal with the age-structured model developed in [1] as follows. First, we calculate the age-structured force of infection from a cross sectional seroprevalence data collected from Caieiras City, a nonimmunized small town in São Paulo State, Brazil [4]. Afterwards, this force of infection is used to estimate the parameters of the contact rate. Once all the parameters of the model are completely characterized, then this model is used to assess the impact of a vaccination schedule restricted on susceptible individuals comprised on an age interval. Observe that this form of vaccination stands between the pulse vaccination [5,6] and vaccination regardless of the age of the individuals [7]. Since the spectral radius results are still under study, here we show only an approximate value for the basic reproduction ratio and the threshold contact rate.

This paper is organized as follows. In Section 2, we transport the model which was introduced in [1], in Section 2.1, we defined the correlated variables with respect to the force of infection and an approximation for the basic reproduction ratio and the threshold vaccination rate are presented in Section 2.2. In Section 3, we present the numerical simulations of the epidemiological values: the natural force of infection in Section 3.1, the estimation of the parameters of the contact rate in Section 3.2, the approximated basic reproduction ratio and the threshold vaccination ratio in Section 3.3 and the force of infection under vaccination and its correlated variables, the average age of the acquisition of the first infection (the age of the infection, hereafter), the rate of new cases of infection (the rate of infection, hereafter), and the risk of Congenital Rubella Syndrome (the risk of CRS, hereafter), in Section 3.4. The results are discussed and commented in Section 4. The results, by applying the spectral radius theory, related to the existence and uniqueness, together with the stability of the integral equation obtained in [1], are left to a further work.

2. THE MODEL

Initially, some results are transported from [1]. The age-structured contact rate developed was of form

$$\beta(a, a') = \beta_0 f_1(a) e^{-b_3|a-a'|}, \tag{1}$$

where β_0 (dimension of time) is the period of exposure, b_3 (dimension of time^{-1}) is the infective contact rate, and the function $f_1(a)$ is

$$f_1(a) = \frac{b_3}{b_2\Gamma(b_1+1)} \frac{(a/b_2)^{b_1} e^{-a/b_2}}{2 - e^{-b_3 a}}, \tag{2}$$

where b_1 is the average number of contacts, b_2 (dimension of time) is togetherness period, and $\Gamma(x)$ is the gamma function.

The age dependent force of infection, with the pattern of contacts and the vaccination rate given by equations (1) and (2), was obtained as Hammerstein equation

$$\lambda(a) = \beta \int_0^L B(a, \zeta) e^{-N(\zeta)} \lambda(\zeta) e^{-\Lambda(\zeta)}\, d\zeta, \tag{3}$$

where L is the upper limit for the duration of human life, $\beta = \beta_0 X_b$ is the transmission coefficient with X_b (dimension of time^{-1}) being the new-born rate and $\Lambda(\zeta) = \int_0^\zeta \lambda(t)\, dt$ and $N(\zeta) = \int_0^\zeta \nu(t)\, dt$ are integral functions. Finally, $B(a, \zeta)$ is the quasikernel given by

$$B(a, \zeta) = f_1(a) \left[f_2(a, \zeta)\theta(\zeta - a) + f_3(a, \zeta)\theta(a - \zeta) \right], \tag{4}$$

with $\theta(x)$ being the step or Heaviside function, and the auxiliary functions $f_2(a,\zeta)$ and $f_3(a,\zeta)$ are given by

$$\begin{aligned} f_2(a,\zeta) &= \frac{\sigma e^{-\mu\zeta} e^{-b_3(\zeta-a)}}{(\mu+\gamma+b_3)(\mu+\sigma+b_3)}, \\ f_3(a,\zeta) &= \frac{\sigma e^{-\mu\zeta} e^{-b_3(a-\zeta)}}{(\mu+\gamma-b_3)(\mu+\sigma-b_3)} - \frac{2\sigma b_3 e^{-\mu a}}{\left[(\mu+\gamma)^2 - b_3^2\right](\sigma-\gamma)} \\ &\quad \times \left\{ e^{-\gamma(a-\zeta)} - \frac{\left[(\mu+\sigma)^2 - b_3^2 - (\sigma-\gamma)(2\mu+\gamma+\sigma)\right] e^{-\sigma(a-\zeta)}}{\left[(\mu+\sigma)^2 - b_3^2\right]} \right\}, \end{aligned} \tag{5}$$

where σ, γ, and μ are, respectively, the incubation, recovery, and mortality rates. Observe that $\beta B(a,\zeta)$ is the kernel when $\nu = 0$.

The integral equation (3) depends on the parameters of the contact rate and the vaccination rate. With respect to the parameters of the contact rate, we fit them based on the seroprevalence curve. In relation to the vaccination rate, since it is usual to vaccinate individuals comprised on an age interval, we consider the expression

$$\nu(a) = \nu\theta(a-a_1)\theta(a_2-a), \tag{6}$$

where a_1 and a_2 are, respectively, the lower and upper bound of the age interval of susceptible individuals vaccinated, and ν is the constant vaccination rate. Hereafter, a_1 will be referred as the lower age vaccinated. Also, we assume that the immunization produces a lifelong immunity, and we neglect the effect of the maternally derived antibodies. This form of controlling strategy stands between the pulse vaccination [5] and vaccination regardless the individuals age [7].

2.1. The Correlated Variables

From the age dependent force of infection $\lambda(a)$, we can calculate the following three correlated variables [7].

(1) The age of the infection is defined by

$$\bar{a} = \frac{\int_0^L a\lambda(a)X(a)\,da}{\int_0^L \lambda(a)X(a)\,da}, \tag{7}$$

where $X(a)$ is the age-specific susceptible individuals in a vaccinated population.

(2) The ratio between the rates of infection restricted on the age interval $[A_1, A_2]$ after and before vaccination strategy is defined by

$$\rho(A_1,A_2) = \frac{\int_{A_1}^{A_2} \lambda(a)X(a)\,da}{\int_{A_1}^{A_2} \lambda_0(a)X_0(a)\,da}, \tag{8}$$

where $X_0(a)$ is the age-specific susceptible individuals in a community without vaccination and $\lambda_0(a)$ is the corresponding natural force of infection. The definite integral gives the incidence rate. The choice of lower (A_1) and upper (A_2) bounds of age interval to analyze this parameter (also the risk of CRS, mainly) is to encompass the average range of age that women usually get pregnant.

(3) The ratio between the risks of CRS on the age interval $[A_1, A_2]$ after and before vaccination strategy is defined by

$$\omega(A_1,A_2) = \frac{\int_{A_1}^{A_2} \lambda(a)X(a)F(a)\,da}{\int_{A_1}^{A_2} \lambda_0(a)X_0(a)F(a)\,da}, \tag{9}$$

where the definite integral is the risk of CRS rate, and $F(a)$ is the fertility function given by

$$F(a) = r_2(a - r_1)e^{-r_2(a-r_1)}\theta(a - r_1), \tag{10}$$

with the parameters r_1 (time) and r_2 (time^{-1}) being, respectively, the minimum age women are able to get pregnant and the fertility loss rate. The fertility function parameters were fitted to the demographic data from the State of São Paulo, Brazil, considering the age of pregnancy [8].

In this paper, we deal with the numerical solution of the integral equation (3). By doing this, we can assess different vaccination strategies. For this reason, we compare the natural force of infection $\lambda_0(a)$ with the new force of infection $\lambda(a)$ resulting from a vaccination strategy taking into account the above three correlated variables.

2.2. Approximated Threshold Values

In this section, we present a method to estimate, approximately, the threshold values. Accordingly in [2,3] the basic reproduction ratio can be related to the spectral radius. If the spectral radius assumes a value greater or equal one, then there is a unique and stable nontrivial force of infection. This result is independent of the choice of norm on the function space considered. However, we are interested in the approximated estimations, since the numerical results related to the spectral radius theory are in study. By the fact that the approximated estimations are heavily dependent on the chosen norm, we will consider three norms: $\|\cdot\|_1$-norm for $L_1[0, L]$, the absolutely integrable functions, $\|\cdot\|_2$-norm for $L_2[0, L]$, the quadratically integrable functions, and sup-norm ($\|\cdot\|_\infty$) for $C[0, L]$, the continuous functions [9]. We apply these three approximated estimations to the age-structured model considering an age dependent contact rate previously developed [1] and then, we compare them.

2.2.1. An approximation for the basic reproduction ratio

Based on the three norms, $\|\cdot\|_1$-norm for $L_1[0, L]$, $\|\cdot\|_2$-norm for $L_2[0, L]$, and sup-norm for $C[0, L]$, we develop an approximate method to estimate the basic reproduction ratio. Observe that the kernel given by expression (4) can be treated as absolutely and quadratically integrable functions, and as a continuous function, on the range $[0, L]$.

Observing the integral equation (3), we note that the trivial solution $\lambda(a) = 0$ is always possible. This is true, if we have $\beta = 0$. Additionally, we must have the trivial solution for lower values of the transmission coefficient. Here, the approximated estimation for the basic reproduction ratio is developed looking only at the trivial solution. We will show that if $0 \le \beta \le \beta^{\text{th}}$, then we can conclude that the trivial solution is the unique stable solution. However, if $\beta > \beta^{\text{th}}$, then we cannot ensure anything.

The integral equation (3), letting $\nu = 0$, has the kernel given by $\beta B(a, \zeta)e^{-\Lambda(\zeta)}$. This equation has the trivial solution as the unique if the mapping $T\lambda(a) = \beta \int_0^L B(a, \zeta)e^{-\Lambda(\zeta)}\lambda(\zeta)\, d\zeta$ is a contraction. Observe that $B(a, \zeta)$ is continuous for $a, \zeta \in [0, L]$, $B(a, \zeta)e^{-\Lambda(\zeta)}$ satisfies a Lipschitz condition with respect to $\lambda(a)$ (see [10] for the proof), and $B(a, \zeta)$ is absolutely or quadratically integrable function. Therefore, if $|\beta|\|B(a, \zeta)\| < 1$, then $\lambda(a) = 0$ is the unique solution (see [9, Chapter 5]). Hence, the under-estimation of the transmission coefficient to ensure the unique solution comes from $\beta^{\text{th}} = \|B(a, \zeta)\|^{-1}$. In relation to the three norms being considered, this can be set as

$$\beta^{\text{th}} = \begin{cases} \left\{\sup\left[\int_0^L |B(a,\zeta)|\, da : 0 < \zeta < L\right]\right\}^{-1}, & \text{for } \|\cdot\|_1\text{-norm}, \\ \left[\int_0^L \int_0^L |B(a,\zeta)|^2\, da\, d\zeta\right]^{-1/2}, & \text{for } \|\cdot\|_2\text{-norm}, \\ \left\{\sup\left[\int_0^L |B(a,\zeta)|\, d\zeta : 0 < a < L\right]\right\}^{-1}, & \text{for sup-norm}. \end{cases} \tag{11}$$

This result shows that, for $\beta < \beta^{\text{th}}$, there is a unique solution (fixed point) for the force of infection according to the contraction mapping theorem, which is $\lambda(a) = 0$.

The approximated estimation provided by the contraction mapping theorem does not provide us with the exact value of β (bifurcation point) at which the trivial solution becomes unstable, and appears the unique nontrivial solution. However, we know that there is $\beta'(> \beta^{\text{th}})$ at which occurs the bifurcation, whose value is obtained when the spectral radius assumes value one. For this reason, the approximated approach provides us with the over-estimation of the basic reproduction ratio, R_0^o, which is given by

$$R_0^o = \frac{\beta}{\beta^{\text{th}}}. \tag{12}$$

Note that the basic reproduction ratio is given by $R_0 = \beta/\beta'$ [2].

2.2.2. An approximation for the threshold vaccination rate

Now, let us consider one community under a vaccination strategy. Generally, a vaccination strategy does not change the pattern of contacts when directly infectious diseases are considered, which is not true regarded to the sexually transmitted diseases [7]. The result given below takes into account the assumption that the pattern of contacts and the transmission coefficient are not altered by the vaccination strategy.

A vaccination strategy may or may not lead to the eradication of the disease. Therefore, one of the main goals of the mathematical model is to furnish the condition for eradication. As preceding results, we are interested in an approximated estimation for the threshold vaccination rate ν^{th}. The integral equation (3), with the vaccination rate given by equation (6), has the kernel given by $\beta B(a,\zeta)e^{-N(\zeta)}e^{-\Lambda(\zeta)}$. This equation has the trivial solution as the unique if the mapping $T\lambda(a) = \beta\int_0^L B(a,\zeta)e^{-N(\zeta)}e^{-\Lambda(\zeta)}\lambda(\zeta)\,d\zeta$ is a contraction. Following the same arguments to obtain the preceding results, if $\|\beta B(a,\zeta)e^{-N(\zeta)}\| < 1$, then $\lambda(a) = 0$ is the unique solution. Hence, the over-estimation of the vaccination rate to ensure the unique solution comes from $\|\beta B(a,\zeta)e^{-N^*(\zeta)}\| = 1$, where $N^*(\zeta)$ is related to ν^{th}. In relation to the three norms being considered, this can be set as the root of equations

$$\begin{aligned}
&\sup\left[\int_0^L \left|\beta B(a,\zeta)e^{-\int_0^\zeta \nu(s)\,ds}\right| da : 0 < \zeta < L\right] - 1 = 0, \qquad \text{for } \|\cdot\|_1\text{-norm},\\
&\left[\int_0^L\int_0^L \left|\beta B(a,\zeta)e^{-\int_0^\zeta \nu(s)\,ds}\right|^2 da\,d\zeta\right]^{1/2} - 1 = 0, \qquad \text{for } \|\cdot\|_2\text{-norm},\\
&\sup\left[\int_0^L \left|\beta B(a,\zeta)e^{-\int_0^\zeta \nu(s)\,ds}\right| d\zeta : 0 < a < L\right] - 1 = 0, \qquad \text{for sup-norm}.
\end{aligned} \tag{13}$$

The solution ν^{th} of the above three equations is the approximated threshold vaccination rate. The result shows that if $\nu > \nu^{\text{th}}$ then, from contraction mapping theorem, there is a unique trivial solution for the force of infection. However, there is $\nu'\,(< \nu^{\text{th}})$ at which the bifurcation occurs, whose value is given by the spectral radius. Therefore, ν^{th} is the over-estimation of the eradication effort. Observe that these threshold vaccination rate formulas are related to the transmission coefficient β. Therefore, if this parameter assumes higher values, then the eradication effort increases (because ν^{th} increases).

The integral equation (13) may or may not have a root, if we consider the vaccination rate given by equation (6). Note that this form of vaccination rate can describe a reasonable intervention regarded childhood infections, where the age interval covered by vaccination must play an important role. Therefore, the eradication effort depends on the lower age vaccinated and on

its range. Hence, the maximum vaccination delay for eradication a_1^{th} can be estimated from the above equations.

In the next section, the above epidemiological parameters with respective numerical methods are presented.

3. EPIDEMIOLOGICAL RESULTS

In this section, a numerical approach is given to the results obtained in the preceding section. The over-estimations of the basic reproduction ratio R_0^o, given by equation (12), and the threshold vaccination rate ν^{th}, given by equation (13), are calculated considering the rubella infection. Rubella serological data [4] comprised a survey of 477 individuals (0–40 years) selected by cluster sampling technique from Caieiras, a small town located in the outskirts of São Paulo city, carried out over the period November 1990 to January 1991. This community has not previously been vaccinated against rubella infection.

Besides the over-estimations of the parameters R_0^o and ν^{th}, we will consider a way to compare how these values can be related to the exact values which could be provided by the spectral radius. This comparison will be done indirectly as follows: we solve numerically the integral equation (3) and we analyze the properties of the correlated variables, especially the age of the infection, given by equation (7).

However, to solve numerically the integral equation (3), we assume that this equation has a unique and stable nontrivial solution, accordingly the results provided by Inaba [3]. Therefore, the age dependent force of infection, which exists and is unique, can be obtained by solving the integral equation (3), with or without a vaccination strategy, by iterative method [11]. To solve this equation numerically, a *FORTRAN* coded program was written. In Appendix A, the numerical methods are briefly described.

For the rubella infection, the incubation and recovery periods are, respectively, $\sigma = 52.0$ years^{-1} and $\gamma = 39.0$ years^{-1}. The mortality rate is set as $\mu = 0.015$ years^{-1}. The parameters of the fertility function are set as $r_1 = 13.0$ years, from the fact that women have a minimum age to get pregnant, and $r_2 = 0.23$ years^{-1}, since the fertility function is zero beyond 50.0 years of age [8]. Also, women usually get pregnant on the age interval from $A_1 = 18.0$ years to $A_2 = 45.0$ years.

3.1. The Natural Force of Infection

The natural force of infection $\lambda_0(a)$ can be estimated from the seroprevalence survey, supposing that the host-parasite system was in equilibrium. There are some methods in the literature about this matter, for instance, the proposal by Farrington [12] and Keiding [13]. Here, we will calculate the force of infection from a fitted seroprevalence curve.

First, from rubella data, the seroprevalence curve, called $s^+(a)$, can be fitted by the maximum likelihood estimation method (Appendix A.1). We choose for the prevalence curve, a polynomial logistic function. Table 1 shows the estimated parameters of a third degree polynomial logistic function.

Table 1. The coefficients of the third degree polynomial logistic function adjusted by the maximum likelihood estimation method.

i	c_i	σ_i^2
0	4.091	0.3044
1	-0.8591 years^{-1}	0.0447
2	0.4232×10^{-1} years^{-2}	0.4554×10^{-3}
3	-0.7485×10^{-3} years^{-3}	0.3097×10^{-6}

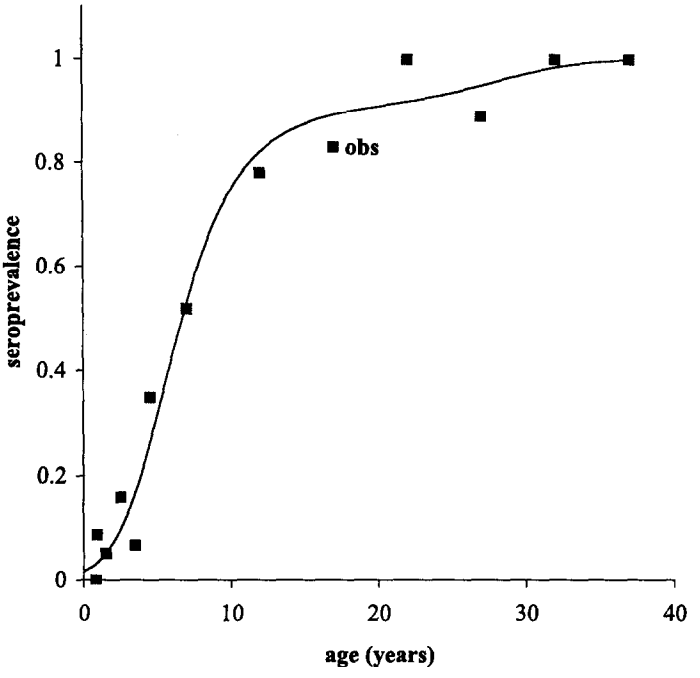

Figure 1. The seroprevalence curve obtained using the estimated parameters given in Table 1.

The corresponding logarithm of the likelihood function is $l = -131.06$. In Figure 1, we show the fitted seroprevalence curve $s^+(a)$.

This seroprevalence curve corresponds to the logistic function with parameters given in Table 1.

Now, the force of infection is derived from $s^+(a)$. Let us consider the age distributed fraction of susceptible individuals $x_0(a)$ $(= X_0(a)/N_0(a)$, where $N_0(a) = e^{-\mu a}$ is the age distribution of individuals in the whole community) in the equilibrium before introduction of vaccination ($\nu = 0$). Note that the equation for the susceptible individuals in the steady state (the first equation of system (1), given in Yang [1]) can be expressed in terms of the fraction $x_0(a)$ as

$$\frac{d}{da}x_0(a) = -\lambda_0(a)x_0(a).$$

Observe that the fraction of the susceptible individuals can be related to the seroprevalence fitting through $x_0(a) = 1 - s^+(a)$, see [4]. Hence, the age dependent natural force of infection is calculated by

$$\lambda_0(a) = \frac{\frac{d}{da}s^+(a)}{1 - s^+(a)}. \tag{14}$$

The force of infection obtained in this manner is shown in Figure 3.

3.2. Estimation of the Model's Parameters

Setting $\nu = 0$ and substituting the calculated $\lambda_0(a)$ in equation (3), then the parameters related to the age-structured contact rate and the transmission coefficient can be determined. The parameters are obtained by considering the convergence of functions theory [9]. In order to do this, we set the force of infection $\lambda_0(a)$, derived from (14), as the target function, and the parameterized force of infection $\lambda_0^p(a)$, given by the integral equation (3), as the trial function.

From the fact that both target and parameterized forces of infection are continuous function on $C[0,L]$, the uniform convergence (sup-norm) or the convergence in the mean ($\|\cdot\|_2$-norm)

can be applied. In the space $C[0,L]$, a sequence of functions $\lambda_0^p(a)$ converges to a function $\lambda_0(a)$ with respect to sup-norm if $\sup\{|\lambda_0^p(a) - \lambda_0(a)| : 0 \leq a \leq L\} \to 0$, which is the condition of uniform convergence. This is not an easy norm to work with. For this reason, the less stringent convergence in the mean,

$$\int_0^L |\lambda_0^p(a) - \lambda_0(a)|^2 \, da \to 0, \tag{15}$$

is adopted, from which a relatively easy methodology can be developed to obtain the model's parameters.

With respect to the force of infection some explanations are needed. As shown elsewhere [4,14], the third degree polynomial presents a variation in the force of infection which has no biological interpretation after a certain age, which corresponds when the seropositivity reaches its asymptote (maximum value). For this reason, we can neglect any fluctuation in the seroprevalence curve occurring in the asymptote. By this rationale, we restrict the range of the age interval on $[0.0, 18.80]$. The force of infection restricted on this age interval is called truncated force of infection (see Figure 3 below), which is used to estimate the model's parameters. Moreover, this age interval comprises 412 individuals, which represents 86.4% of the sample.

We calculate the convergence in the mean, given by condition (15), by applying the nonlinear least square estimation techniques (Appendix A.2). By this technique, we are calculating the minimum of equation (15). For this purpose, the force of infection $\lambda_0(a)$ was divided into equally spaced 604 points on the age interval $[0.0, 18.80]$. The parameters which minimizes equation (15) are shown in Table 2.

Table 2. The parameters of the age-structured contact rate calculated by the convergence in the mean.

j	b_j
1	1.494
2	9.370 years
3	0.2163 years^{-1}
β	5331.0

In Figure 2, the age-structured contact rate constructed using the set of parameters given in Table 2 is shown.

Figure 2 shows the age-structured contact rate on $[0.0, 45.0]$, instead of the restricted age interval. This extension is reasonable because a high number of potentially infective contacts among individuals occurs at age school, around ten years (close to estimated b_2), and the infective contacts among elder individuals drop nearly to zero.

A methodology was developed to retrieve the effective age-structured contact rate $\beta(a, a')$ from the natural force of infection $\lambda_0(a)$. But, in reality, the force of infection is the final result (the "effect", measurable) of the infection that disseminates according to the patterns of contacts among individuals (the "cause", incommensurable). Therefore, uncertainties arise when the age dependent force of infection, which is a one-dimensional entity, is being related to the age-structured contact rate, which is a bidimensional entity [7]. For instance, the convergence sum obtained with the parameters given in Table 2 is $S^2(604) = 4.43 \times 10^{-3}$. However, there is another set of parameters with lower convergence sum, $S^2(604) = 3.42 \times 10^{-3}$. Notwithstanding, this set, given by $b_1 = 0.9183$, $b_2 = 427.5$ years, $b_3 = 0.3741$ years^{-1}, and $\beta = 0.202 \times 10^7$, was rejected, since the value of b_2 is higher.

From the truncated force of infection, we obtained the model's parameters. Now, the force of infection provided by the model can be calculated by iterating the integral equation (3) setting $\nu = 0$. In this case, we have a particular iteration (see the general case in Appendix A.3) given by

$$\lambda_0^{n+1}(a) = \beta \int_0^L B(a, \zeta) \lambda_0^n(\zeta) e^{-\int_0^\zeta \lambda_0^n(s)\, ds} d\zeta, \qquad n = 0, 1, \ldots,$$

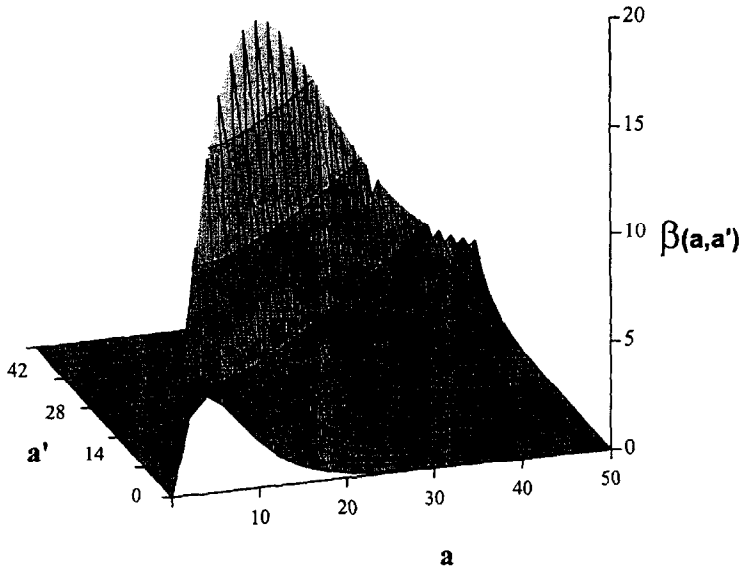

Figure 2. The effective age-structured contact rate ($\beta(a, a')$ in years^{-1} and a and a' in years) obtained using parameters given in Table 2.

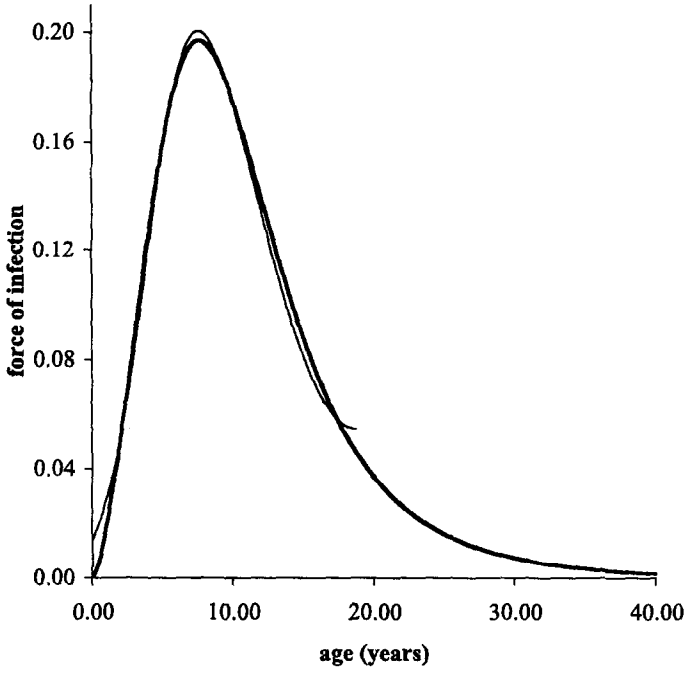

Figure 3. The truncated (thin curve) and model's (thick curve) natural forces of infection (years^{-1}).

where $\lambda_0^0(a)$ is the extension to the age interval $[0.0, 45.0]$ of the truncated $\lambda_0(a)$ as $\lambda_0^0(a) = \lambda_0(a)$ if $a \leq 18.8$ and $\lambda_0^0(a) = \lambda_0(18.8)$, otherwise.

Figure 3 shows both the truncated and the model's force of infection.

As cited before, the truncated force of infection is valid on the age interval $[0.0, 18.80]$. On this age interval, the average age of the acquisition of the first infection, obtained from equation (7), is $\bar{a}_0 = 6.88$ years. Moreover, the model's force of infection, extended to the age interval $[0.0, 45.0]$, gives for the age of the infection, $\bar{a}_0 = 7.41$ years, higher than that provided by the truncated

one. In all the following simulations, the extended age interval is adopted.

3.3. Estimation of the Approximated Threshold Values

The value of the transmission coefficient, $\beta = 5330.90$ from the last row of Table 2, is fixed to obtain the approximated threshold values. In Table 3, the approximated threshold transmission coefficient β^{th}, calculated from equation (11), and the over-estimation of the basic reproduction ratio ($R_0^o = \beta/\beta^{\text{th}}$) are presented for two norms (Appendix A.4).

Table 3. The over-estimation of the basic reproduction ratio for $\|\cdot\|_2$- and sup-norms.

β^{th}	a_{sup} (years)	R_0^o	norm
1389.77	–	3.84	$\|.\|_2$
1448.30	12.45	3.68	sup

For the sup-norm, Table 3 shows the age a_{sup}, which corresponds to the maximum value of $\int_0^L |B(a,\zeta)|\, d\zeta$ at which β^{th} was found. The $\|\cdot\|_1$-norm is not considered here (see Appendix A.4).

When dealing with the threshold vaccination rate, it is interesting to relate the vaccination rate to the proportion covered by vaccination, since the latter is easier to understand. The proportion related to the vaccination rate can be calculated taking into account only the age interval being vaccinated. Then, we have

$$p(\nu) = 1 - \frac{\int_{a_1}^{a_2} X(a)\, da}{\int_{a_1}^{a_2} X_0(a)\, da}. \tag{16}$$

Nevertheless, almost all individuals older than six months are susceptibles [4], then, in early ages, the susceptible individuals can be approximated by the total population. By doing $X_0(a) \simeq X_b e^{-\mu a}$ and $X(a) \simeq X_b e^{\nu a_1} e^{-(\mu+\nu)a}$ for $a_1 \le a \le a_2$, a relation between vaccination rate and the proportion of the effectively vaccinated is obtained by

$$p(\nu) \sim 1 - \frac{\mu}{\mu+\nu} \frac{1 - e^{-(\mu+\nu)(a_2-a_1)}}{1 - e^{-\mu(a_2-a_1)}}\,. \tag{17}$$

Equation (17) gives the effective proportion of susceptible individuals covered by vaccination on the age interval a_1 to a_2, disregarding the fraction of susceptible individuals infected naturally. The approximation (17) becomes more and more imprecise when a_1 and a_2 are increased.

By the form of the vaccination rate given in equation (6), the eradication effort depends on the lower age vaccinated a_1 and on its range. In order to analyze the effects of the range of age interval covered by vaccination, and to estimate the maximum vaccination delay a_1^{th} to have eradication, two possible vaccination strategies are presented.

First, the effects of the range of age interval covered by vaccination is analyzed. To do this, the lower age vaccinated a_1 is fixed and the range is increased by varying a_2. Figure 4 shows, for $\|\cdot\|_2$-norm and sup-norm, the approximated threshold vaccination rate ν^{th}, calculated from equation (13).

Figure 4 shows, for $\|\cdot\|_2$-norm (thick curves) and sup-norm, a similar behaviour, except that the proportion corresponding to the threshold vaccination rate is slightly higher in $\|\cdot\|_2$-norm. This kind of strategy can describe mass vaccination campaign, which involves a broad age interval. Note that in mass vaccination, if the lower age vaccinated is sufficiently small, then there are no threshold values.

Second, the effects of earlier and later vaccination programs are analyzed. To do this, the age interval covered by the vaccination program $a_2 - a_1$ is fixed, and the lower age vaccinated a_1 is delayed. Figure 5 shows, for $\|\cdot\|_2$-norm and sup-norm, the approximated threshold vaccination rate ν^{th} and a_1^{th}.

For $\|\cdot\|_2$-norm (thick curves), the maximum vaccination delay to have eradication a_1^{th} lies on the semi-open interval $[4.49, 4.50)$, and for sup-norm, $[5.06, 5.07)$. The results are given in

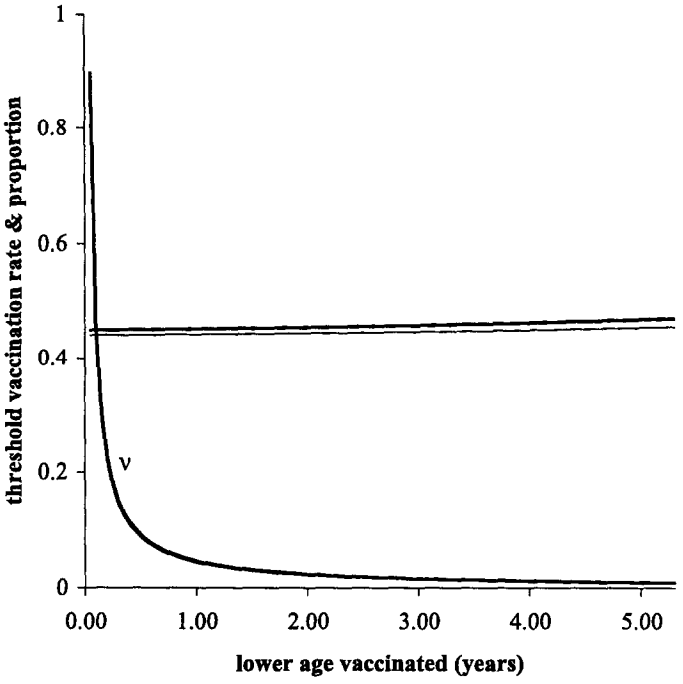

Figure 4. The threshold vaccination rate (with symbol ν and $\times 30$ years^{-1} for both norms which are practically coincident) and the corresponding proportion (without symbol) vaccinated. We fixed $a_1 = 0$ years and varied a_2, for $\|\cdot\|_2$-norm (thick curves) and sup-norm (thin curves).

intervals due to the numerical simulations. If $a_1 > a_1^{\text{th}}$, then the disease cannot be eradicated. From Figure 5, when $a_1 < a_1^{\text{th}}$, there is a well-defined ν^{th}. From the fact that ν^{th} is the over-estimation of the threshold vaccination rate, then a_1^{th} is the under-estimation of the threshold lower age vaccinated.

In this section, all the threshold values, β^{th} (and R_0^o), ν^{th} and a_1^{th} are approximated values. These values are heavily dependent on the norm considered. These values are compared with the results obtained in the next section.

3.4. Vaccination Strategies Assessment

The new equilibrium force of infection, after the introduction of a vaccination strategy, with its correlated variables are presented in this section.

Since the correlated variables are given as ratios, we present these values found before vaccination: the age of the infection $\bar{a}_0 = 7.41$ years, from equation (7), the rate of infection $\rho_0(A_1, A_2) = 0.03102$ years^{-1}, from the denominator of equation (8), and the risk of CRS $\omega_0(A_1,A_2) = 0.001114$ years^{-1}, from the denominator of equation (9).

First, we present the effects of a vaccination strategy varying the range of the age interval of susceptible individuals vaccinated. The new forces of infection fixing the lower age vaccinated a_1 and enlarging the range of age covered by vaccination by increasing a_2 are shown in Figure 6, for: $[1.0, 2.0]$ Figure 6a and $[1.0, 10.0]$ Figure 6b.

The figures show that, as p increases, the peak of the force of infection is shifted rightwardly (to higher ages), and once a certain proportion is attained, thereafter the shift is reversed to the left (to lower ages). The proportion at where the shift to the right stops and then reverses to the left can be taken as the threshold proportion, and above it, the disease can be considered eradicated. The range of the shift to the right is slowed if the age interval covered by vaccination is increased. It is observed that the threshold proportion to have eradication obtained in this

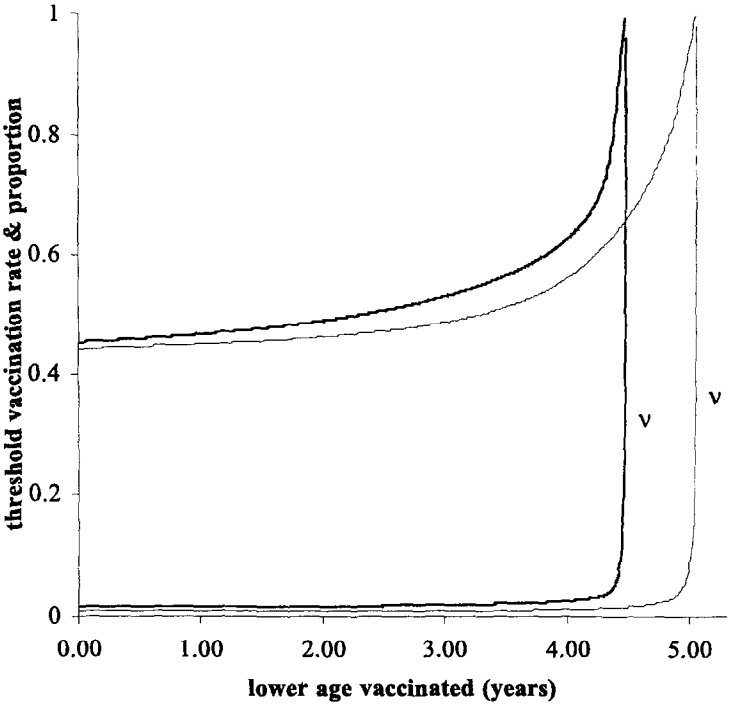

Figure 5. The approximated threshold vaccination rate (with symbol ν and $\times 100$ years^{-1} for $\|\cdot\|_2$-norm and $\times 170$ years^{-1} for sup-norm) and the corresponding proportion (without symbol) vaccinated. We fixed $a_2 - a_1 = 1.0$ year and varied a_1, for $\|\cdot\|_2$-norm (thick curves) and sup-norm (thin curves). The threshold lower age vaccinated to have eradication is the vertical asymptote.

manner situates on the interval $[0.40, 0.45]$, which is close to the range $[0.44, 0.50]$ calculated from the contraction mapping theorem (see Figure 5).

From the age dependent force of infection, the ratios of the correlated variables are shown in Figure 7.

Figure 7 sheds more light on the reversion phenomenon, i.e., the reverse of the shift of the peak of the force of infection from right to left. Figure 7a displays a feature different from Figure 7b. In latter figure, the ratios of the rate of infection and the risk of CRS above the threshold proportions are zero, but in the former, the ratio of the age of the infection increases and abruptly goes to zero (a mathematical artefact which was removed). Hence, Figure 7a shows that the reverse phenomenon is related to the nonphysical situation: a nontrivial force of infection resulted in zero valued rate of infection (and the risk of CRS), but a decreasing phase in the age of the infection. From these figures, the eradication proportion can be estimated situating on the range $[0.38, 0.48]$.

Observe that the eradication proportion obtained by the model (Figure 5) is an over-estimation. This range, in comparison with the numerical simulations, given in Figures 6 and 7, provided us with higher values for the lower and upper bounds, as expected. Consequently, if we take into account both the reverse phenomenon (related to the force of infection) and the p-axis crossing (related to the correlated variables), then the eradication proportion can be set as the union of intervals estimated by them, that is, $[0.38, 0.48]$.

With respect to the above reversion phenomenon in the force of infection and abruptly decaying in the age of the infection, we can find quite similar behaviours when we consider a constant contact rate. In this modeling, the force of infection decreases continuously, passes through zero and then, assumes negative value. The behaviour of the force of infection affects the age of the infection as follows. The positive force of infection corresponds to an increasing phase for the age of the infection, and to the negative force of infection, a decreasing phase for the age of the infection [15].

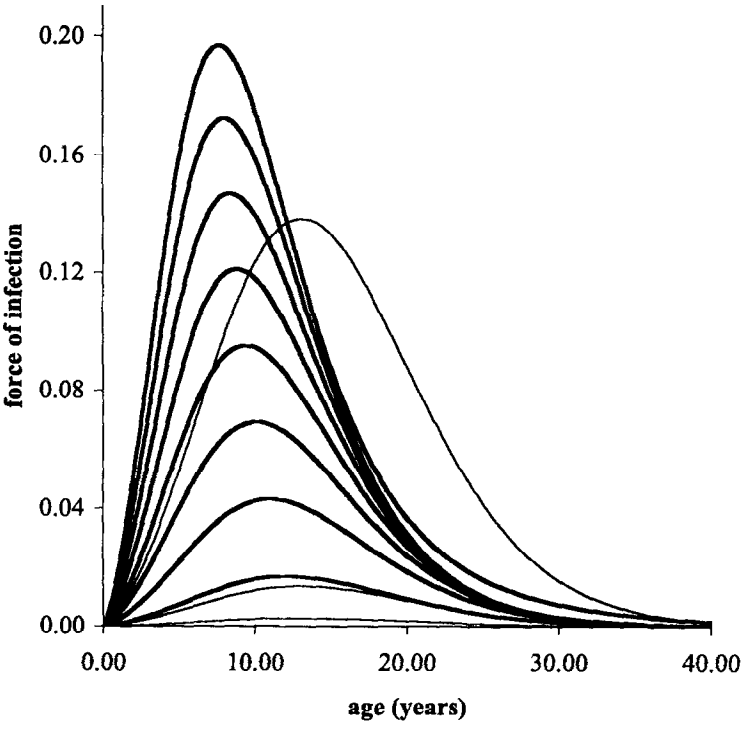

(a)

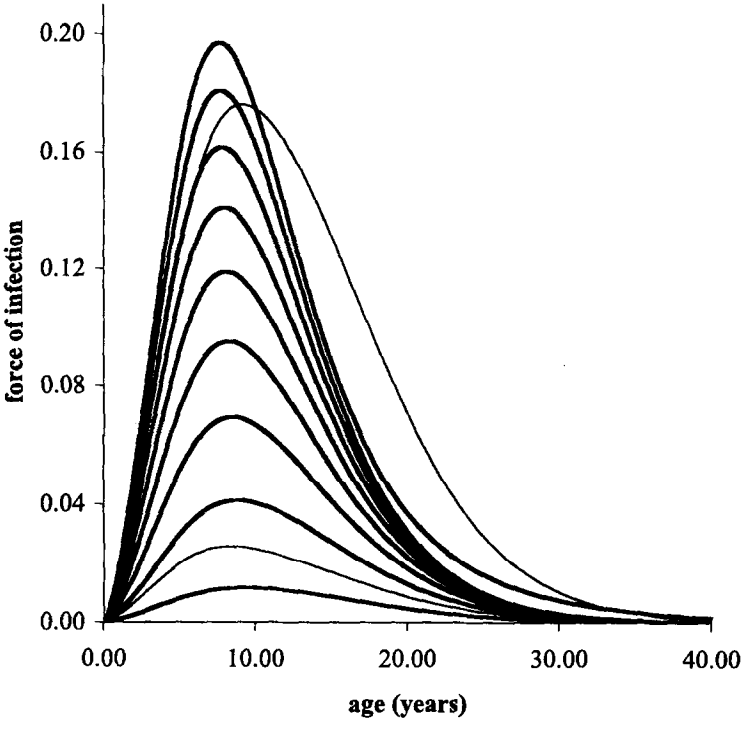

(b)

Figure 6. The force of infection (years^{-1}) for different proportion vaccinated. (a) refers to the age interval [1.0, 2.0], with the thin curves corresponding to three last proportion vaccinated multiplied by 5.0×10^8. (b) refers to the age interval [1.0, 10.0], with the thin curves corresponding to two last proportion vaccinated multiplied by 2.0×10^9. For both figures, the proportions are $p = 0$, 0.05, 0.1, 0.15, 0.2, 0.25, 0.3, 0.35, 0.4, 0.45, and 0.5 (from top to bottom).

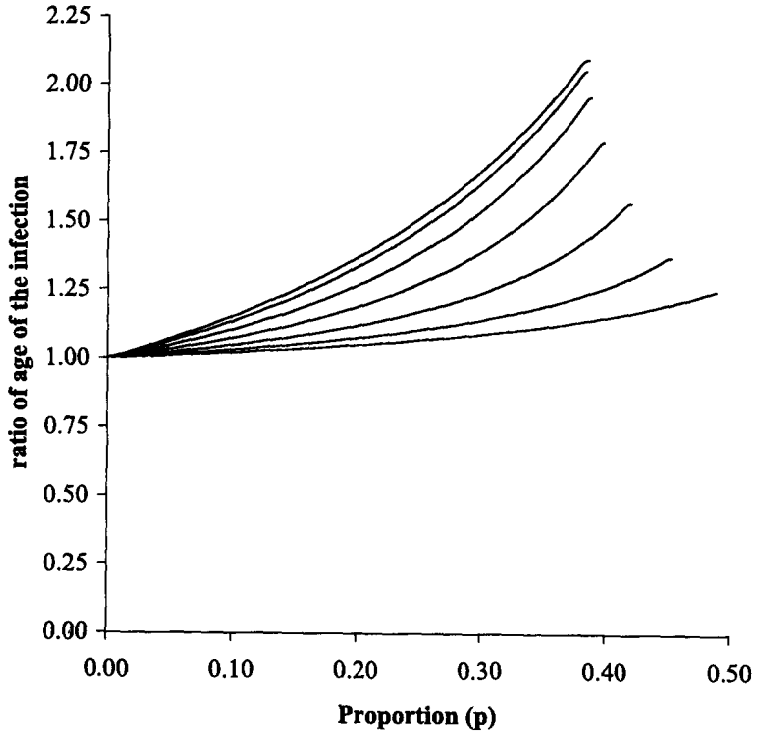

(a)

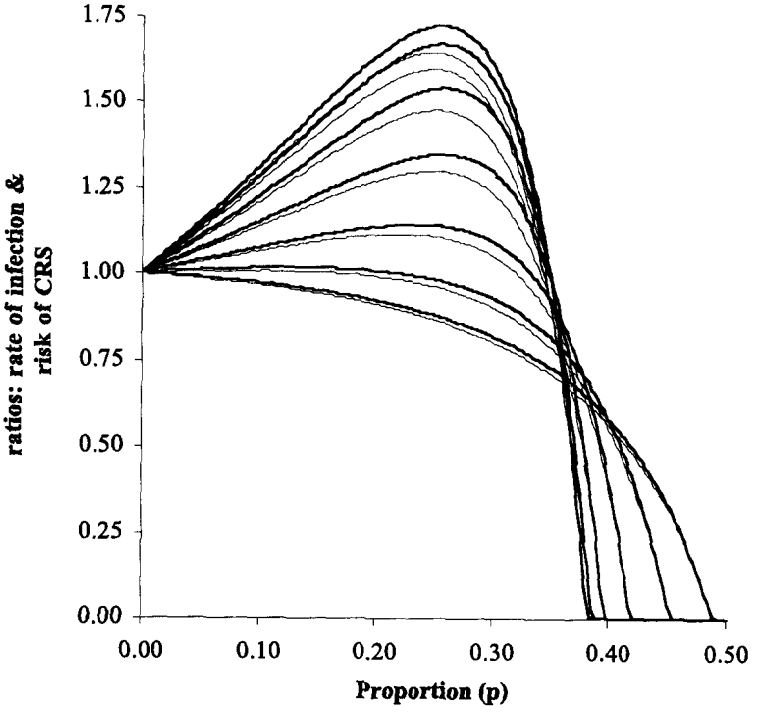

(b)

Figure 7. The ratios of the correlated variables as a function of the proportion vaccinated, fixing $a_1 = 1.0$ year and varying a_2. (a) refers to the age of the infection. (b) refers to the rate of infection (thick curves) and to the risk of CRS (thin curves). To both figures, the vaccinated age intervals are: [1.0, 2.0], [1.0, 4.0], [1.0, 6.0], [1.0, 8.0], [1.0, 10.0], [1.0, 12.0], and [1.0, 14.0] (from top to bottom, in region of small p).

Second, the effects of earlier and later vaccination strategy is assessed. The new equilibrium force of infection, fixing the age interval $a_2 - a_1$ and delaying the lower age vaccinated a_1, is shown in Figure 8, for: $[4.0, 5.0]$ Figure 8a and $[14.0, 15.0]$ Figure 8b.

Figure 8a shows also the reversion phenomenon, but the range of displacement is lower than that shown in Figure 6. Quite the same results are observed if the age interval vaccinated $[5.0, 6.0]$ is used. However, if the age interval vaccinated $[5.5, 6.5]$ is considered, the results are quite the same as those shown in Figure 8a, except that the peak of the force of infection shifts continuously to the left, without having the reversion phenomenon. This remains valid if the vaccination scheme is delayed by increasing the lower age vaccinated, as shown in Figure 8b. In this case, the vaccination proportion does not affect the ascendent phase in the force of infection, but the descending phase is strongly diminished. Therefore, the estimation of the lower age vaccinated, by numerical simulations, is located on the open age interval (5.0,5.5).

Figure 9 shows the correlated variables of the new age dependent force of infection when fixing the age interval vaccinated and delaying the vaccination strategy.

When a vaccination strategy can eradicate the disease, we observe that the approximate estimation of the proportion vaccinated to have eradication becomes worse with the increasing of the lower age vaccinated. For instance, for $a_1 = 1.0$ years, we have around 50% to the over-estimation (Figure 5) of the proportion vaccinated to lead to eradication, but the simulation (Figure 9b) shows that this proportion is around 40%. When a vaccination strategy does not eradicate the disease, then the ratios of the rate of infection and the risk of CRS have same displays (Figure 9b, three bottom curves). It is also observed that, if the vaccination is delayed, it is not possible to eradicate the disease, but the three correlated variables take values lower than one for all proportions vaccinated. Figure 9a (three bottom curves) shows the ratio of the age of the infection decreasing monotonically. It corresponds to the continuous leftwardly displacement of the peak of force of infection. The result related to the age of the infection shows that the well-established paradigm, that the average age of the acquisition of the first infection increases with vaccination, is not always true.

We compare the threshold lower age vaccinated a_1^{th} obtained by the simulation with the approximated values. Observe that the approximated value for a_1^{th}, provided by the $\|\cdot\|_2$-norm is lower than that predicted by the simulation, while the result provided by sup-norm is located on the range given by the simulation.

Finally, we remark that the approximated estimation for R_0^a and ν^{th} are over-estimations and a_1^{th} is under-estimation. These approximated estimations were obtained by a direct application of the contracting mapping theorem. Note that these results are relatively close to those provided by the simulations (in terms of the reversion phenomenon in the force of infection and the abruptly decaying behaviour in the age of the infections). But, we must bear in mind that, in any eradication strategy, an extra amount of effort must be considered to take into account the factor security. Therefore, the over-estimations of R_0^a and ν^{th} and under-estimation of a_1^{th} are interesting and useful results to be considered in a vaccination strategy.

4. DISCUSSION

An advantage of the approach presented here is its capacity of representing a community pattern of contacts linked to the natural force of infection through the population's seroprevalence data. The method proposed in this paper takes into account the force of infection to estimate all the model's parameters (of the pattern of contacts and transmission coefficient), and consequently, describes a refined age distribution of the infection, which greatly differs from constant contact rate models.

A kind of pattern of contacts was developed here. We used probabilistic event, considering demographic and social obligations, to construct a probability function to describe the contacts made among individuals. However, the infective contact was restricted to the Laplace distri-

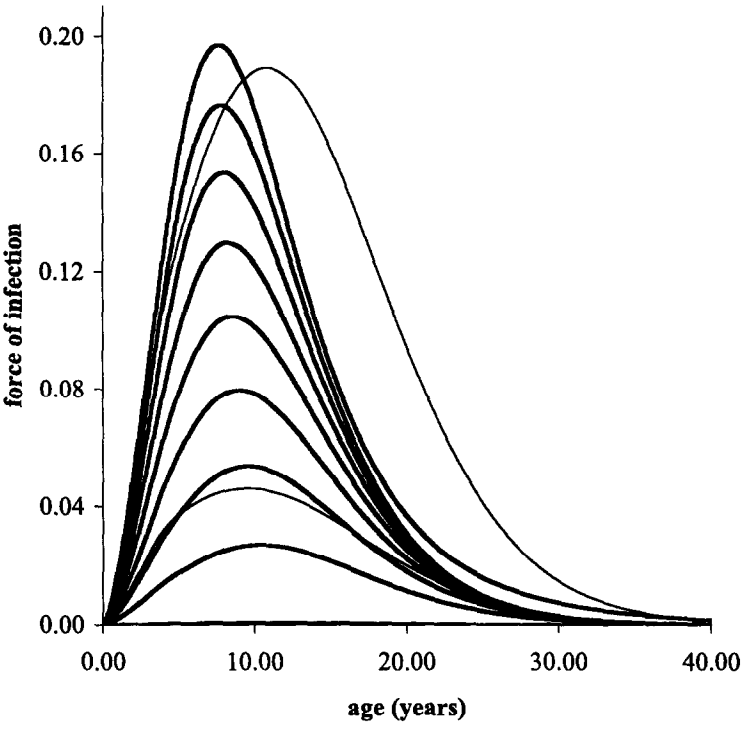

(a)

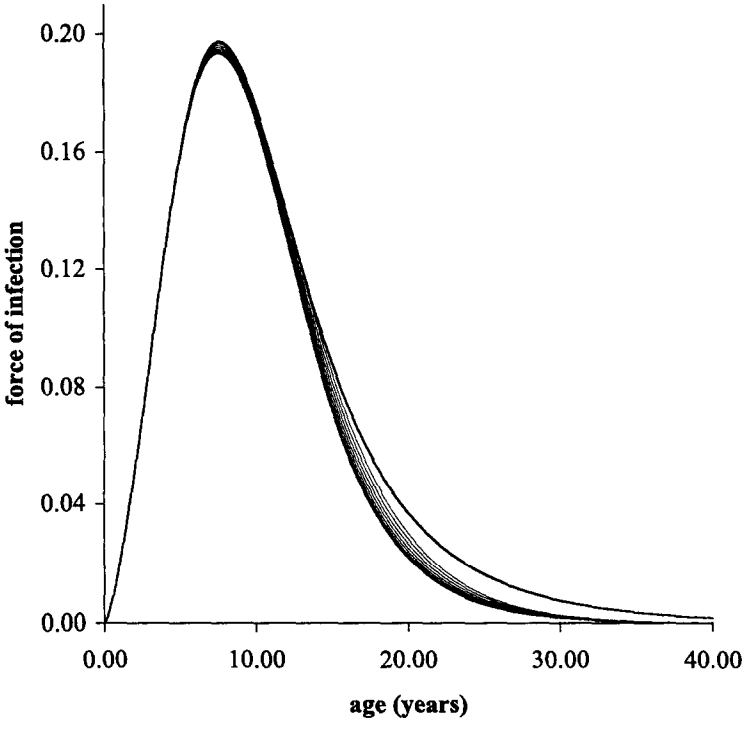

(b)

Figure 8. The force of infection (years^{-1}) for different proportion vaccinated. (a) refers to the age interval [4.0, 5.0] and p = 0, 0.05, 0.1, 0.15, 0.2, 0.25, 0.3, 0.35, 0.45, and 0.5 (from top to bottom). The thin curves corresponding to two last proportion vaccinated multiplied by 4.0×10^9. (b) refers to the age interval [14.0, 15.0] and p = 0, 0.1, 0.2, 0.3, 0.4, 0.5, 0.6, 0.7, 0.8, 0.9, and 1.0 (from top to bottom).

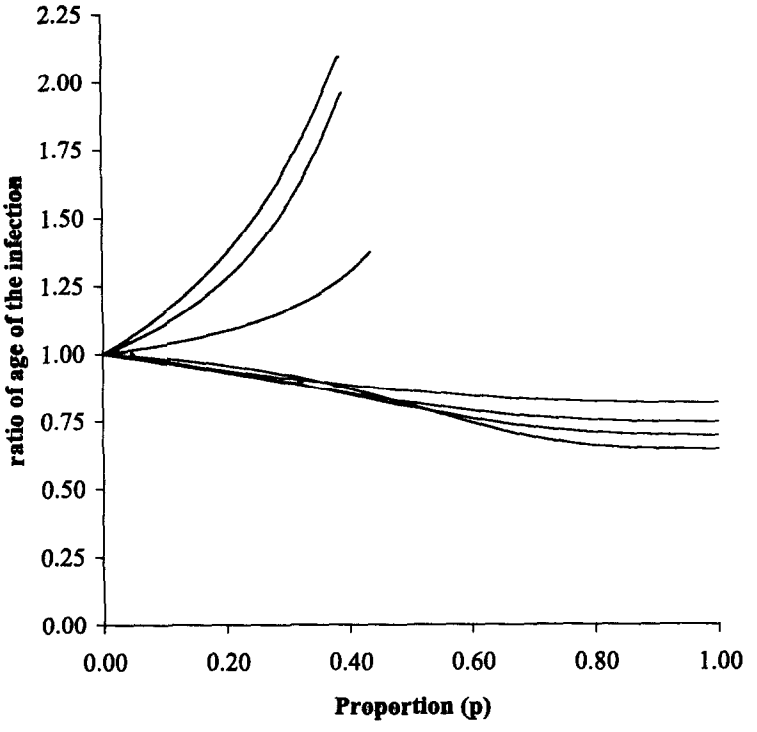

(a)

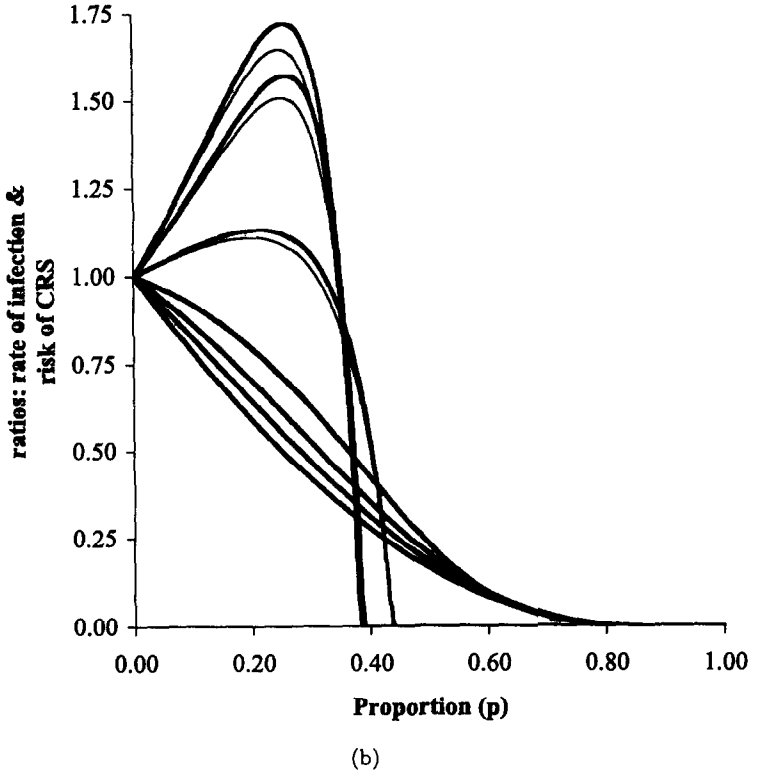

(b)

Figure 9. The ratios of the correlated variables as a function of the proportion vaccinated, fixing $a_2 - a_1 = 1.0$ year and varying a_1. (a) refers to the age of the infection. (b) refers to the rate of infection (thick curves) and to the risk of CRS (thin curves), and both are coincident when there is not eradication. For both figures, the vaccinated age intervals are: [1.0, 2.0], [3.0, 4.0], [5.0, 6.0], [7.0, 8.0], [8.0, 9.0], [9.0.10.0], and [11.0, 12.0] (from top to bottom, in region of small p).

bution. This restriction resulted, when dealing with contraction mapping theorem, that the $\|\cdot\|_1$-norm was not applicable. But $\|\cdot\|_2$-norm and sup-norm provided valuable approximated estimations.

The pattern of contacts is a very important feature to take into account when designing vaccination strategies. However, the results shown in Table 3 can lead to misleading conclusions: the introduction of heterogeneity in the contact among individuals diminishes the eradication effort. The constant contact rate model, with an estimation for the basic reproduction ratio higher than the value in this model, leads to disease eradication irrespective of the age interval chosen to be vaccinated [7]. Even though the basic reproduction ratio has lower estimate than that provided by the constant contact rate model [15], the age-structured contact rate model shows that the eradication effort is not facilitated. This is due, as can be observed from the above simulations, to the fact that the eradication condition is attained only if an appropriate age interval could be chosen. Also, the constant contact rate modeling is only a crude approximation of the reality.

The main theoretical results were obtained from contraction mapping theorem. The approximated estimations from theoretical considerations were compared with the numerical results for the force of infection and its correlated variables. The comparisons were based on the classical constant contact rate modeling: the reversion phenomenon in age-structured model was linked with the negative force of infection in the constant contact rate modeling. The results are in a close relation. Moreover, the contraction mapping theorem gives us an easy way to estimate approximately the important epidemiological parameters R_0^o, ν^{th}, and a_1^{th}

Finally, the vaccination rate on an age interval can be seen as an alternative to a pulse vaccination. From this kind of vaccination, we note that the vaccination on a broad age interval, like $[1.0, 10.0]$, can be used to describe the mass vaccination [8]. On the other hand, the early vaccination, like the age interval $[1.0, 2.0]$, corresponds to the vaccination schedule in the U.S.A., and the delayed vaccination, like the age interval $[14.0, 15.0]$, to that in course in Great Britain [16]. Also, this kind of vaccination rate showed that the increase in the average age of the acquisition of the first infection is not always true. Nevertheless, the approximated estimations provided in this paper can be a useful tool to epidemiologists when these values are taken into account carefully, since they can be understood as the true values added with security term.

APPENDIX
NUMERICAL METHODS

The numerical solutions of the following mathematical expressions were transposed to Fortran codes and commands.

A.1. Seroprevalence Fitting

The seroprevalence data are described by a logistic function,

$$s^+(a;\mathbf{c}) = \frac{1}{1+e^{\text{pol}\,(a,\mathbf{c})}}, \tag{18}$$

with $\text{pol}(a,\mathbf{c}) = \sum_{i=0}^{m} c_i a^i$ being a polynomial of degree m. The set of parameters $\mathbf{c}$ of the above function was fitted by the maximum likelihood estimation method. For this, the logarithm of the likelihood function, given by

$$l(\mathbf{c}) = \sum_{i=1}^{n} \left\{ d_i \ln\left[s^+(a_i;\mathbf{c})\right] + D_i \ln\left[1 - s^+(a_i;\mathbf{c})\right] \right\} \tag{19}$$

is used, where d_i and D_i are the number of serologically positives and negatives in the age a_i, respectively. The set of parameters maximizes the likelihood function at

$$\mathbf{y}(\mathbf{c}) = \frac{\partial l(\mathbf{c})}{\partial \mathbf{c}} = \sum_{i=1}^{n} \left[\frac{d_i}{s^+(a_i;\mathbf{c})} - \frac{D_i}{1 - s^+(a_i;\mathbf{c})} \right] \frac{\partial}{\partial \mathbf{c}} s^+(a_i;\mathbf{c}) = \mathbf{0}, \tag{20}$$

because the inverse of the covariance matrix, neglecting the second derivatives of the logistic function in relation to the parameters [17], given by

$$\Sigma^{-2}(\mathbf{c}) = -\frac{\partial^2 l(\mathbf{c})}{\partial \mathbf{c}^2} \sim \sum_{i=1}^{n} \left\{ \frac{d_i}{[s^+(a_i;\mathbf{c})]^2} + \frac{D_i}{[1-s^+(a_i;\mathbf{c})]^2} \right\} \left[\frac{\partial}{\partial \mathbf{c}} s^+(a_i;\mathbf{c}) \right]^2 \tag{21}$$

is negatively defined. The estimator $\hat{\mathbf{c}}$ that obeys (20) is the value searched.

Due to the approximation in the second derivative, the maximum likelihood estimator is obtained by the Levenberg-Marquardt nonlinear fitting method [17]. This method is the modified Newton-Raphson method, where the increments in the new set of parameters are given by

$$\Sigma_{LM}^{-2}(\mathbf{c}) = \begin{cases} \sigma^{-2}(\mathbf{c})(1+\varepsilon), & \text{on the diagonal,} \\ \eta^{-2}(\mathbf{c}), & \text{off the diagonal,} \end{cases} \tag{22}$$

where σ^2 and η^2 are, respectively, the variance and covariance of matrix (21), and ε is an auxiliary parameter. The initial guess is provided by the least square estimation method.

A.2. Estimation of the Model's Parameters

Equation (3), with $\nu = 0$, relates the natural force of infection $\lambda_0(a)$ and the model's parameters, through the convergence in the mean (15). As pointed out in the main text, the estimation of the four parameters of the model can be done by minimizing the convergence function (15). If this function is integrated using the trapezoidal rule with equal age-subintervals, then the nonlinear least square method can be applied. Therefore, the minimization of the convergence in the mean is furnished if, disregarding the constant age-subinterval of integration, the convergence sum

$$S^2(\theta) = \sum_{i=1}^{M} \left[\beta \int_0^L B(a_i,\zeta;\theta)\lambda_0(\zeta) e^{-\Lambda_0(\zeta)}\, d\zeta - \lambda_0(a_i) \right]^2 \tag{23}$$

is minimized in relation to the set of parameters $\theta = [b_1\ b_2\ b_3\ \beta]^\top$, where $B(a,\zeta;\theta)$ is the kernel (4) and M is the number of points the natural age dependent force of infection derived from seroprevalence fitting is subdivided. The set of parameters minimizes (23) at

$$\begin{aligned} \mathbf{y}(\theta) = \frac{1}{2}\frac{\partial S^2(\theta)}{\partial \theta} = \sum_{i=1}^{M} & \left[\beta \int_0^L B(a_i,\zeta;\theta)\lambda_0(\zeta) e^{-\Lambda_0(\zeta)}\, d\zeta - \lambda_0(a_i) \right] \\ & \times \beta \int_0^L \frac{\partial}{\partial \theta} B(a_i,\zeta;\theta)\lambda_0(\zeta) e^{-\Lambda_0(\zeta)}\, d\zeta = \mathbf{0}, \end{aligned} \tag{24}$$

because the inverse of the covariance matrix, disregarding the second derivatives of the kernel in relation to the parameters,

$$\Sigma^{-2}(\theta) = \frac{1}{2}\frac{\partial^2 S^2(\theta)}{\partial \theta^2} \sim \sum_{i=1}^{M} \left[\beta \int_0^L \frac{\partial}{\partial \theta} B(a_i,\zeta;\theta)\lambda_0(\zeta) e^{-\Lambda_0(\zeta)}\, d\zeta \right]^2 \tag{25}$$

is positively defined. Again the Levenberg-Marquardt method is applied. The set of parameters $\hat{\theta}$ that obeys (24) is the estimated parameters of the model. The analytical expressions for $\frac{\partial}{\partial \theta} B(a_i,\zeta;\theta)$ were omitted.

A.3. Solution By Iterations

The integral equation (3), when the vaccination strategy is applied in a community, can be solved numerically by the iterative method, that is,

$$\lambda_n(a) = \beta \int_0^L B(a,\zeta) e^{-N(\zeta)} \lambda_{n-1}(\zeta) e^{-\Lambda_{n-1}(\zeta)}\, d\zeta, \qquad n = 0,\ 1, \ldots, \tag{26}$$

where $\lambda_0(a)$ is the force of infection provided by the model, and the halt condition is

$$\left\{ \int_0^L |\lambda_n(a) - \lambda_{n-1}(a)|^2 \right\}^{1/2} \leq \varepsilon_{\text{tol}}. \tag{27}$$

Here $\varepsilon_{\text{tol}} \leq 10^{-6}$ was used, which decreases with increasing proportion covered by vaccination. The numerical integration method used was the *extended Simpson's rule*.

A.4. Threshold Calculations

The two integro-transcendental equations given by (11) and (13) are solved to find the threshold values. These equations are handled in the following manner.

(a) The threshold value (11) needs to calculate the integration of the square of the kernel for $\|\cdot\|_2$-norm and the supremum of the kernel for sup-norm. The square of the kernel has an analytical expression which is so extensive and then, was omitted. However, the integration can be calculated applying the Gaussian quadratures. The supremum is calculated using the Brent maximization method.

(b) The threshold vaccination rate (13) needs to calculate the integrations $\int_0^L |\beta B(a,\zeta) e^{-N(\zeta)}|^2 \, d\zeta$ for $\|.\|_2$-norm and $\int_0^L |\beta B(a,\zeta) e^{-N(\zeta)}| \, d\zeta$ for sup-norm. In both norms, the roots are calculated using the Brent root finding method.

In relation to the $\|\cdot\|_1$-norm, the disease can be eradicated if

$$\text{Sup}\left\{\int_0^L \left|\beta B(a,\zeta) e^{-N(\zeta)}\right| da : 0 \le \zeta < L\right\} < 1. \tag{28}$$

But this condition is never satisfied. Note that, if we set $\zeta = 0$, then we have $\int_0^L |\beta B(a,0)| \, da = 1.12$, and whatever the vaccination rate is, it is always higher than unity.

REFERENCES

1. H.M. Yang, Directly transmitted infections modeling considering an age-structured contact rate, *Mathl. Comput. Modelling* (to appear).
2. D. Greenhalgh, Vaccination campaigns for common childhood diseases, *Math. Biosc.* **100**, 201–240, (1990).
3. H. Inaba, Threshold and stability results for an age-structured epidemic model, *J. Math. Biol.* **28**, 411–434, (1990).
4. R.S. Azevedo Neto, A.S.B. Silveira, D.J. Nokes, H.M. Yang, S.D. Passos, M.R.A. Cardoso and E. Massad, Rubella seroepidemiology in a non-immunized population of São Paulo state, Brazil, *Epidemiol. Infect.* **113** (1), 161–173, (1994).
5. H.W. Hethcote, Optimal ages of vaccination for measles, *Math. Biosc.* **89**, 29–52, (1988).
6. H.M. Yang, Modelling vaccination strategy against directly transmitted diseases using a series of pulses, *Jour. Biol. Systems* **6** (2), 187–212, (1998).
7. R.M. Anderson and R.M. May, *Infectious Diseases of Humans: Dynamics and Control*, Oxford University Press, Oxford, (1991).
8. E. Massad, M.N. Burattini, R.S. Azevedo Neto, H.M. Yang, F.A.B. Coutinho and D.M.T. Zanetta, A model-based design of vaccination strategy against Rubella in a non-immunized community, *Epidemiol. Infect.* **112**, 579–594, (1994).
9. D.H. Griffel, *Applied Functional Analysis*, John Wiley & Sons, New York, (1981).
10. F.A.B. Coutinho, E. Massad, M.N. Burattini, H.M. Yang and R.S. Azevedo Neto, Effects of vaccination programmes on transmission rates of infections and related threshold conditions for control, *IMA J. Math. App. Med. Biol.* **10**, 187–206, (1993).
11. F.G. Tricomi, *Integral Equations*, Dover, New York, (1985).
12. C.P. Farrington, Modelling forces of infection for measles, mumps, and rubella, *Stat. Med.* **9**, 953–967, (1990).
13. N. Keiding, Age-specific incidence and prevalence: A statistical perspective, *J. Royal Statistic. Soc. A.* **154**, 371–412, (1991).
14. D.J. Nokes, R.M. Anderson and M.J. Anderson, Rubella epidemiology in South East England, *J. Hyg.* **96**, 291–304, (1986).
15. H.M. Yang, Impacto da Vacinação nas Infecções de Transmissão Direta—Epidemiologia Através de Modelo Matemático (port.), Thesis, IMECC—UNICAMP, (1997).
16. R.M. Anderson and R.M. May, Vaccination against rubella and measles: Quantitative investigations of different policies, *Cambridge J. Hygiene* **90**, 259–325, (1983).
17. W.H. Press, B.P. Flannery, S.A. Teukolsky and W.T. Vetterling, *Numerical Recipes: The Art of Scientific Computing (FORTRAN Version)*, Cambridge University Press, Cambridge, (1989).